Acoust. Sci. & Tech. **23**, 6 (2002)

PAPER

Active modal control of sound fields by finite element modeling and H_∞ control theory

Toshiya Samejima and Daisuke Yamamoto

Department of Acoustic Design, Kyushu Institute of Design, 4–9–1, Shiobaru, Minami-ku, Fukuoka, 815–8540 Japan

(*Received 22 November 2001, Accepted for publication 10 June 2002*)

Abstract: A new method of feedback control of sound fields that minimizes the total acoustic energy in a sound field of any shape excited by an unknown disturbance is presented. The proposed method is based on the finite element method and H_∞ control theory, and achieves both robust performance and high stability. The structure of the acoustic plant is formulated such that the H_∞ norm of the system transfer function expresses the total acoustic energy in the sound field. Computer simulations verify that the damping of a sound field can be increased without leading to instabilities of the closed loop system. It is also verified that the resonant peaks in the frequency spectrum of the total acoustic energy can be attenuated in the low-frequency range involved in the nominal model of the plant without exciting the residual mode dynamics in the high-frequency range. The control performance can be tuned by adjusting the weighting factor. Using this method, it is possible to dynamically alter the characteristics of a sound field.

Keywords: Active noise control, Feedback control, Finite element method, H_∞ control theory

PACS number: 43.50.Ki, 43.55.Br, 43.55.Ka

1. INTRODUCTION

Active control of sound fields, which involves the use of electro-acoustic transducers to drive the output of an acoustic plant to a desired output, is useful in low-frequency applications because passive methods such as installing sound absorbers are not effective at low frequencies. The technology of active control of sound fields has been developed and studied by a number of researchers, primarily involving the use of methods based on inverse filtering of the transfer functions from sound sources to receiving points in a sound field and simulating the desired transfer functions as strictly as possible. However, in addition to dealing with the transfer functions from sound sources to receiving points, it is necessary to regard a full sound field as a plant and to develop a method to alter plant dynamics.

The full sound field can be treated as a plant by expressing a sound field mathematically with a wave equation. Nelson *et al.* developed feedforward control of sound fields using frequency response functions based on modal analysis of a wave equation so as to minimize the total acoustic potential energy in an enclosure [1–3]. Ise *et al.* formulated a control method that accounted for actuator dynamics using the boundary element method for the same control objective [4]. However, both of these control methods require the reference signal of the primary source to be available and the sound field to be harmonic. Thus, the effectiveness of such control cannot be guaranteed when the primary source cannot be measured or is uncorrelated. In addition to this, these methods are not intended to alter plant dynamics.

The dynamics between a sound source and a receiving point in a sound field are significantly affected by the poles of the transfer function between them. By introducing a feedback loop into the plant under study, the poles of the transfer function can be controlled, thereby controlling the modal response of the plant. Clark *et al.* proposed a feedback control system based on direct rate feedback control for control of the modal damping ratio of acoustic modes [5]. In their system, the sound pressure at a microphone collocated with a loudspeaker is fed back through the electro-acoustic transducer. Using mode theory, they described the stability of the sound field into which their control system was introduced and reported the simulation results for globally damping the acoustic response of an enclosure.

Several studies on the application of modern control theory based on the state-space method for active control of sound fields have been published. Dohner *et al.* [6] and Bai *et al.* [7] developed active noise control systems using linear quadratic optimal control. In their system, the full sound field was regarded as a plant, however it was assumed that the modal parameters for describing the sound field in state space were known theoretically or experimentally. Dohner *et al.* also derived a method that was not based on mode theory for constructing a state equation for a sound field but accounted for every mode [8]. However, their analysis was applied to a one-dimensional problem for simplicity.

In a previous paper [9], we derived a state-space description of a sound field from an inhomogeneous wave equation using the finite element method (FEM). This allows the sound field to be treated without relying on any kind of shape that may have unknown modal parameters, and alleviates the need to identify the modal parameters of the sound field experimentally. We investigated control of the poles of the transfer function in the sound field using state feedback control based on the linear quadratic Gaussian (LQG) for suppression of reverberation in a room, and demonstrated that the control method was used effectively to globally damp the acoustic response of a room.

However, when this control method is applied to a real sound field and real-time feedback control is practically carried out, an inevitable problem related to modeling errors occurs. In general, a feedback controller is designed for a nominal model of a plant. When this feedback controller is introduced into the real plant, modeling errors construct an extra closed loop, which may cause instabilities of the whole closed loop system. Since this control method uses FEM to model a sound field as a plant, modeling errors are caused by several factors: 1) considering a sound field to be a linear time-invariant system; 2) idealization of boundary conditions; 3) discritization of space; 4) approximation of the exact solution by a trial function that is a polynomial series; 5) numerical calculation with a digital computer. These modeling errors coexist between a real sound field and its nominal model. In particular, the modeling error due to approximation of the exact solution by a trial function is a fundamental problem. Although a real sound field, which is a distributed system, requires an infinite number of modes to completely describe its behavior, FEM can express only a finite number of low-frequency modes of the sound field depending on the number of terms of the trial function. Thus, the feedback controller of this method ignores the high-frequency modes of the sound field. However, these high-frequency modes behave as residual mode dynamics because the sensor outputs are contaminated by the high-frequency modes and the feedback control commands excite the high-frequency modes. These are called observation spillover and control spillover, respectively, and must be taken into account in the design of the feedback controller. This problem has been investigated in the field of active control of vibrations in mechanically flexible systems that are also distributed systems. Balas showed that the combined effect of observation and control spillover can result in instabilities of the closed loop system, and also showed that while instabilities cannot occur if the observation spillover is eliminated, the residual modes excited by the control commands degrade the control performance [10]. Thus, a design method that calculates the optimal feedback controller in terms of both performance and stability of the closed loop system is needed.

In the present study, we apply H_∞ control theory to the feedback control of sound fields. H_∞ control theory is an effective scheme for designing feedback controllers that accommodate both performance and stability in an optimal and robust manner. We have developed a new active control method that alters the dynamic characteristics of a sound field with any shape while meeting the requirements of robust performance and robust stability through a combination of FEM and H_∞ control theory. For application of the control method to minimizing the total acoustic energy in a room, the structure of the acoustic plant is formulated such that the H_∞ norm of the system transfer function, which is used as the performance index of the H_∞ control problem, expresses the total acoustic energy in the sound field. This study tries to overcome instabilities of the closed loop system or degradation of the control performance, especially due to residual mode dynamics. In general, a real system involves all kinds of modeling errors, which cannot be divided clearly. Thus, as a preliminary study, the theoretical formulation of the proposed control method is confirmed by computer simulations, in which a real sound field is simulated by a theoretical solution of the inhomogeneous wave equation. According to this, one can clearly discuss the effect of residual mode dynamics on the proposed control system. The effects of other modeling errors and experimental verification are needed for future work.

2. H_∞ CONTROL THEORY

In this section, a brief review of H_∞ control theory is given. The details of the theory can be found in the literature [11–13]. Here, the standard H_∞ control problem and its solution are summarized, and two typical control problems that can be solved by H_∞ control theory and can be related to problems of feedback control of sound fields are described.

2.1. Standard H_∞ Control Problem and Its Solution

In H_∞ control theory, all control structures are described using a generalized control framework as shown

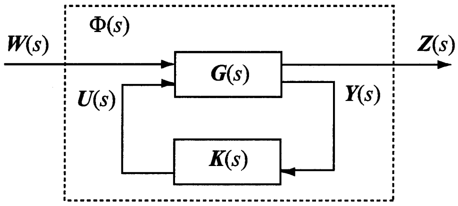

Fig. 1 Generalized control framework.

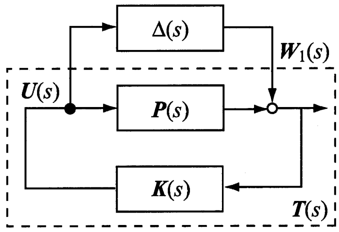

Fig. 2 Closed loop system with additive plant uncertainty.

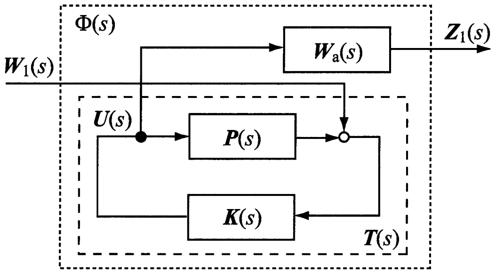

Fig. 3 System configuration for robust stability problem.

in Fig. 1. The framework is constructed by a generalized plant $\boldsymbol{G}(s)$ and a feedback controller $\boldsymbol{K}(s)$. $\boldsymbol{\Phi}(s)$ is the transfer function from the disturbance $\boldsymbol{W}(s)$ to the controlled variable $\boldsymbol{Z}(s)$, thus,

$$\boldsymbol{Z}(s) = \boldsymbol{\Phi}(s)\boldsymbol{W}(s). \tag{1}$$

The rationale of H_∞ control is to minimize the H_∞ norm of $\boldsymbol{\Phi}(s)$ by carrying out appropriate feedback control $\boldsymbol{U}(s) = \boldsymbol{K}(s)\boldsymbol{Y}(s)$, thereby minimizing $\boldsymbol{Z}(s)$. $\boldsymbol{U}(s)$ and $\boldsymbol{Y}(s)$ are the control input to the plant and the measured output from the plant, respectively. As it is difficult to find an optimal feedback controller $\boldsymbol{K}(s)$, a suboptimal feedback controller $\boldsymbol{K}(s)$ is used that makes $\boldsymbol{\Phi}(s)$ asymptotically stable and that satisfies

$$\|\boldsymbol{\Phi}(s)\|_\infty < \gamma, \tag{2}$$

where γ is a given positive number. Finding such $\boldsymbol{K}(s)$ is called the standard H_∞ control problem and can be analytically solved using various H_∞ algorithms developed by researchers of automatic control.

In this paper, the state space approach to the H_∞ control problem developed by Sampei *et al.* [14] is employed. The standard H_∞ control problem is solved using a state-space description for a generalized plant $\boldsymbol{G}(s)$ expressed as follows:

$$\begin{cases} \dot{\boldsymbol{x}} = \boldsymbol{A}\boldsymbol{x} + \boldsymbol{B}_1\boldsymbol{w} + \boldsymbol{B}_2\boldsymbol{u} \\ \boldsymbol{z} = \boldsymbol{C}_1\boldsymbol{x} + \boldsymbol{D}_{11}\boldsymbol{w} + \boldsymbol{D}_{12}\boldsymbol{u} \\ \boldsymbol{y} = \boldsymbol{C}_2\boldsymbol{x} + \boldsymbol{D}_{21}\boldsymbol{w} \end{cases}. \tag{3}$$

By solving two Riccati equations derived from the above equations, one can obtain a feedback controller $\boldsymbol{K}(s)$ expressed as the following state-space description.

$$\begin{cases} \dot{\boldsymbol{x}}_c = \boldsymbol{A}_c\boldsymbol{x}_c + \boldsymbol{B}_c\boldsymbol{y} \\ \boldsymbol{u} = \boldsymbol{C}_c\boldsymbol{x}_c \end{cases} \tag{4}$$

2.2. Robust Stabilization Problem

Generally, it is difficult to model a plant accurately. Modeling errors are inevitable when a plant is identified either theoretically or experimentally. Perturbations of a plant may also occur due to variations in physical conditions such as temperature, humidity, and boundary conditions. These bring about deviations of the real plant from its nominal model called plant uncertainties, which affect the stability of the closed loop system.

Figure 2 shows a closed loop system containing a plant uncertainty. Here, $\boldsymbol{P}(s)$ is a nominal plant model, $\boldsymbol{K}(s)$ is a feedback controller, $\boldsymbol{T}(s)$ is the transfer function from $\boldsymbol{W}_1(s)$ to $\boldsymbol{U}(s)$, and $\boldsymbol{\Delta}(s)$ is an additive uncertainty. To ensure stability of the closed loop system against this plant uncertainty, the following robustness condition derived from the small gain theorem must be satisfied.

$$\|\boldsymbol{W}_a(s)\boldsymbol{T}(s)\|_\infty < 1, \tag{5}$$

where $\boldsymbol{W}_a(s)$ satisfies

$$\sigma_{\max}[\boldsymbol{\Delta}(j\omega)] \le \sigma_{\max}[\boldsymbol{W}_a(j\omega)], \quad \forall\omega \in R, \tag{6}$$

where $\sigma_{\max}[\cdot]$ denotes the maximum singular value. Finding $\boldsymbol{K}(s)$ that satisfies Eq. (5) is called the robust stability problem. If the closed loop system shown in Fig. 2 is transformed into the system shown in Fig. 3 using $\boldsymbol{W}_a(s)$, the transfer function from $\boldsymbol{W}_1(s)$ to $\boldsymbol{Z}_1(s)$ is given by

$$\boldsymbol{Z}_1(s) = \boldsymbol{W}_a(s)\boldsymbol{T}(s)\boldsymbol{W}_1(s). \tag{7}$$

Thus, this problem can be treated as the standard H_∞ control problem, where $\boldsymbol{\Phi}(s) = \boldsymbol{W}_a(s)\boldsymbol{T}(s)$ and $\gamma = 1$.

2.3. Disturbance Attenuation Problem

Figure 4 shows a closed loop system excited by a disturbance $\boldsymbol{W}_2(s)$. $\boldsymbol{S}(s)$ is the transfer function from $\boldsymbol{W}_2(s)$ to the output $\boldsymbol{Y}(s)$ of the system. By minimizing the gain of $\boldsymbol{S}(s)$, the response of $\boldsymbol{Y}(s)$ to $\boldsymbol{W}_2(s)$ can be reduced. Thus, if the nominal performance condition expressed as

$$\|\boldsymbol{W}_s(s)\boldsymbol{S}(s)\|_\infty < 1 \tag{8}$$

is satisfied under an appropriate weighting function $\boldsymbol{W}_s(s)$,

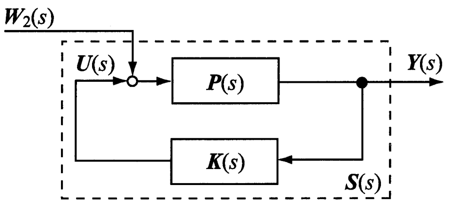

Fig. 4 Closed loop system excited by disturbance.

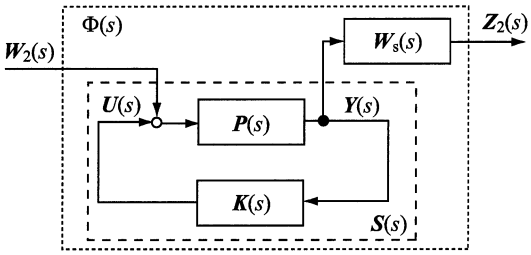

Fig. 5 System configuration for disturbance attenuation problem.

disturbance attenuation can be achieved. Finding $\boldsymbol{K}(s)$ that satisfies Eq. (8) is called the disturbance attenuation problem. If the closed loop system shown in Fig. 4 is transformed into the system shown in Fig. 5 using $\boldsymbol{W}_\mathrm{s}(s)$, the transfer function from $\boldsymbol{W}_2(s)$ to $\boldsymbol{Z}_2(s)$ is given by

$$\boldsymbol{Z}_2(s) = \boldsymbol{W}_\mathrm{s}(s)\boldsymbol{S}(s)\boldsymbol{W}_2(s). \tag{9}$$

Thus, one can treat also this problem as the standard H_∞ control problem, where $\boldsymbol{\Phi}(s) = \boldsymbol{W}_\mathrm{s}(s)\boldsymbol{S}(s)$ and $\gamma = 1$.

2.4. Mixed Sensitivity Problem

In most cases the feedback controller is designed with regard to both robustness and performance. If the condition

$$\left\| \begin{bmatrix} \boldsymbol{W}_\mathrm{a}(s)\boldsymbol{T}(s) \\ \boldsymbol{W}_\mathrm{s}(s)\boldsymbol{S}(s) \end{bmatrix} \right\|_\infty < 1 \tag{10}$$

is satisfied, both the stability of the closed loop system against a plant uncertainty and disturbance attenuation, i.e., robust performance, can be achieved. Finding $\boldsymbol{K}(s)$ that satisfies Eq. (10) is called the mixed sensitivity problem. Figure 6 shows the closed loop system, combining the system shown in Fig. 3 and the system shown in Fig. 5. It is easy to see that this problem can be solved as the standard H_∞ control problem by treating this system as the generalized control framework shown in Fig. 1.

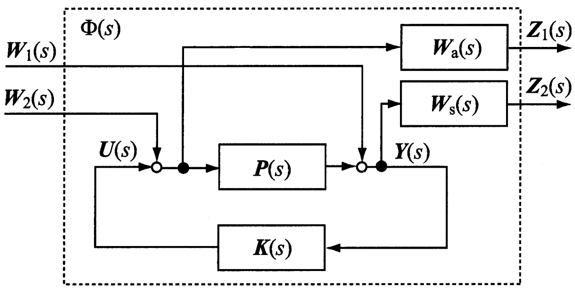

Fig. 6 System configuration for mixed sensitivity problem.

3. THE PROPOSED H_∞ CONTROL SYSTEM

3.1. State-Space Description of a Sound Field

In this section, to describe a sound field (i.e., a control plant) in state space, a state equation for a sound field is constructed using FEM.

The inhomogeneous wave equation related to velocity potential ϕ is expressed as follows:

$$\nabla^2\phi - \frac{1}{c^2}\frac{\partial^2\phi}{\partial t^2} = -q, \tag{11}$$

where c is the speed of sound in the fluid and q is the distribution of the strength of sound sources. Applying FEM to the above equation with area Ω and boundary Γ, the following can be obtained [15,16].

$$\boldsymbol{M}\ddot{\boldsymbol{\phi}} + \boldsymbol{D}\dot{\boldsymbol{\phi}} + \boldsymbol{K}\boldsymbol{\phi} = \boldsymbol{f}u, \tag{12}$$

with

$$\begin{cases} M_{ij} = \dfrac{1}{c^2}\displaystyle\iiint_\Omega N_i N_j dV \\ D_{ij} = -\rho \displaystyle\iint_\Gamma \dfrac{1}{z} N_i N_j dS \\ K_{ij} = \displaystyle\iiint_\Omega \operatorname{grad} N_i \cdot \operatorname{grad} N_j dV \\ f_i = \displaystyle\iiint_\Omega q N_i dV \end{cases},$$

where $\boldsymbol{\phi}$ is a vector with components of velocity potential ϕ at each node, u is the strength of the sound source, ρ is the density of the fluid, z is the normal acoustic impedance of the boundary surface, and N_i is the interpolation function of the i-th node. Equation (12) can be transformed into a state-space description as follows:

$$\begin{cases} \dot{\boldsymbol{x}}_\mathrm{p} = \boldsymbol{A}_\mathrm{p}\boldsymbol{x}_\mathrm{p} + \boldsymbol{B}_\mathrm{w}\boldsymbol{w}_2 + \boldsymbol{B}_\mathrm{p}u \\ \boldsymbol{y}_\mathrm{e} = \boldsymbol{C}_\mathrm{e}\boldsymbol{x}_\mathrm{p} \\ y_\mathrm{p} = \boldsymbol{C}_\mathrm{p}\boldsymbol{x}_\mathrm{p} + w_1 \end{cases}, \tag{13}$$

with

$$\boldsymbol{A}_\mathrm{p} = \begin{bmatrix} \boldsymbol{0} & \boldsymbol{I} \\ -\boldsymbol{M}^{-1}\boldsymbol{K} & -\boldsymbol{M}^{-1}\boldsymbol{D} \end{bmatrix}, \boldsymbol{x}_\mathrm{p} = \begin{Bmatrix} \boldsymbol{\phi} \\ \dot{\boldsymbol{\phi}} \end{Bmatrix}, \boldsymbol{B}_\mathrm{p} = \begin{Bmatrix} \boldsymbol{0} \\ \boldsymbol{M}^{-1}\boldsymbol{f} \end{Bmatrix},$$

$$\boldsymbol{C}_\mathrm{p} = \{\boldsymbol{0} \quad 0\cdots0 \quad \rho \quad 0\cdots0\},$$

where $\boldsymbol{I}$ is the identity matrix. The formulation of $\boldsymbol{B}_\mathrm{w}$ depends on the kind of disturbance $\boldsymbol{w}_2$ that is considered. In this paper, it is assumed that each state variable, i.e., each component of $\boldsymbol{x}_\mathrm{p}$, is independently excited by each component of $\boldsymbol{w}_2$. Hence, $\boldsymbol{B}_\mathrm{w} = \boldsymbol{I}$. The above state equation includes two output equations that generate the controlled variable and the measured signal, respectively. $\boldsymbol{C}_\mathrm{p}$ of one of the output equations is formulated such that the output y_p of the system becomes the sound pressure

$p = \rho \partial\phi/\partial t$ at a point in the sound field.

For a practical implementation of the feedback controller, electro-acoustic transducers are required to measure and excite a sound field. Thus, the dynamics of the electro-acoustic transducers must be considered to represent the dynamics of the acoustic plant more accurately. This is accomplished by coupling the matrix equation by FEM of the sound field with the equation of motion of the electro-acoustic transducer. In a previous paper, on the basis of this procedure, we presented a method to model an acoustic plant including mechanism of a loudspeaker [17]. Ignoring the dynamics of the electro-acoustic transducers causes a modeling error, which was referred to as the modeling error due to idealization of boundary conditions in the literature [18]. Since this modeling error is beyond the scope of this study, only a state-space description of an acoustic plant not including actuator and measurement dynamics will be discussed for the simplicity.

3.2. Formulation for Minimization of Total Acoustic Energy

Here, the matrix $\boldsymbol{C}_{\rm e}$ of the other output equation is formulated such that the controlled variable becomes the total acoustic energy in the sound field. The weighting functions $\boldsymbol{W}_{\rm a}(s)$ and $\boldsymbol{W}_{\rm s}(s)$ are also formulated for the stability of the closed loop system against the plant uncertainty, which cannot be modeled by FEM.

Using the state space variables $\boldsymbol{x}_{\rm p}$ in the state-space description given by Eq. (13), the instantaneous total acoustic energy in the sound field is expressed as follows:

$$
\begin{aligned}
E &= \frac{\rho}{2}\sum_n \left\{\left(\frac{\partial\phi}{\partial x}\right)_n^2 + \left(\frac{\partial\phi}{\partial y}\right)_n^2\right\} V_n + \frac{\rho}{2c^2}\sum_n \left(\frac{\partial\phi}{\partial t}\right)_n^2 V_n \\
&= \boldsymbol{\phi}^{\rm T}\frac{\rho}{2}\boldsymbol{K}\boldsymbol{\phi} + \dot{\boldsymbol{\phi}}^{\rm T}\frac{\rho}{2}\boldsymbol{M}\dot{\boldsymbol{\phi}} \\
&= \begin{Bmatrix} \boldsymbol{\phi} \\ \dot{\boldsymbol{\phi}} \end{Bmatrix}^{\rm T} \begin{bmatrix} \frac{\rho}{2}\boldsymbol{K} & \boldsymbol{0} \\ \boldsymbol{0} & \frac{\rho}{2}\boldsymbol{M} \end{bmatrix} \begin{Bmatrix} \boldsymbol{\phi} \\ \dot{\boldsymbol{\phi}} \end{Bmatrix} \\
&= {\boldsymbol{x}_{\rm p}}^{\rm T}\boldsymbol{R}\boldsymbol{x}_{\rm p},
\end{aligned}
\tag{14}
$$

where $(\phi)_n$ denotes the velocity potential in the n-th element and V_n is the volume of the n-th element. $\boldsymbol{R}$ can be decomposed as $\boldsymbol{R} = \boldsymbol{L}\boldsymbol{L}^{\rm T}$ because $\boldsymbol{R}$ is a positive semi-definite symmetric matrix. The formulation

$$\boldsymbol{C}_{\rm e} = \boldsymbol{L}^{\rm T} \tag{15}$$

sets the L_2 norm of the other output $\boldsymbol{y}_{\rm e}$ of the system equal to the square root of the time integral of the total acoustic energy, as shown in the following.

$$
\begin{aligned}
\|\boldsymbol{y}_{\rm e}\|_2 &= \left(\int_0^\infty {\boldsymbol{y}_{\rm e}}^{\rm T}(t)\boldsymbol{y}_{\rm e}(t)dt\right)^{1/2} \\
&= \left(\int_0^\infty \{\boldsymbol{C}_{\rm e}\boldsymbol{x}_{\rm p}(t)\}^{\rm T}\{\boldsymbol{C}_{\rm e}\boldsymbol{x}_{\rm p}(t)\}dt\right)^{1/2} \\
&= \left(\int_0^\infty {\boldsymbol{x}_{\rm p}}^{\rm T}(t){\boldsymbol{C}_{\rm e}}^{\rm T}\boldsymbol{C}_{\rm e}\boldsymbol{x}_{\rm p}(t)dt\right)^{1/2} \\
&= \left(\int_0^\infty {\boldsymbol{x}_{\rm p}}^{\rm T}(t)\boldsymbol{L}\boldsymbol{L}^{\rm T}\boldsymbol{x}_{\rm p}(t)dt\right)^{1/2} \\
&= \left(\int_0^\infty E(t)dt\right)^{1/2}
\end{aligned}
\tag{16}
$$

On the other hand, if a system $\boldsymbol{S}(s)$ is stable and its initial condition is 0, its H_∞ norm is expressed as follows:

$$
\begin{aligned}
\|\boldsymbol{S}(s)\|_\infty &= \sup\{\sigma_{\max}[\boldsymbol{S}(j\omega)] : \omega \in [0, \infty)\} \\
&= \sup\{\|\boldsymbol{y}(s)\|_2 : \|\boldsymbol{w}(s)\|_2 = 1\},
\end{aligned}
\tag{17}
$$

where $\boldsymbol{y}(s)$ and $\boldsymbol{w}(s)$ are the output and input of $\boldsymbol{S}(s)$ [13]. Thus, the formulation Eq. (15) relates the H_∞ norm of the transfer function from $\boldsymbol{w}_2$ to $\boldsymbol{y}_{\rm e}$ to the time integral of the total acoustic energy in the sound field.

When a sound field is modeled as a plant using FEM, the dynamics of the nominal model of the plant are not accurate in the high-frequency range. In this range, the wavelengths are not sufficiently long compared to the size of the finite elements. Thus, $W_{\rm a}(s)$ should be formulated such that it expresses the plant uncertainty. For simplicity, $W_{\rm a}(s)$ is approximated as a high-pass filter expressed in state space as follows:

$$
\begin{cases} \dot{\boldsymbol{x}}_{\rm a} = \boldsymbol{A}_{\rm a}\boldsymbol{x}_{\rm a} + \boldsymbol{B}_{\rm a}u \\ z_1 = \boldsymbol{C}_{\rm a}\boldsymbol{x}_{\rm a} + D_{\rm a}u \end{cases}.
\tag{18}
$$

As the mixed sensitivity problem is a trade-off between the robust stabilization problem and the disturbance attenuation problem, it is reasonable that $\boldsymbol{W}_{\rm s}(s)$ is chosen as a low-pass filter:

$$
\begin{cases} \dot{\boldsymbol{x}}_{\rm s} = \boldsymbol{A}_{\rm s}\boldsymbol{x}_{\rm s} + \boldsymbol{B}_{\rm s}\boldsymbol{y}_{\rm e} \\ \boldsymbol{z}_2 = \alpha\boldsymbol{C}_{\rm s}\boldsymbol{x}_{\rm s} \end{cases},
\tag{19}
$$

where a scalar gain α is introduced as the weighting factor for tuning the control performance. The feedback controller designed for the mixed sensitivity problem will try to minimize both the output z_1 of $W_{\rm a}(s)$ and the output $\boldsymbol{z}_2$ of $\boldsymbol{W}_{\rm s}(s)$. z_1 approximates the output of plant uncertainty driven by the control command u. $\boldsymbol{z}_2$ represents the low-pass filtered $\boldsymbol{y}_{\rm e}$ related to the total acoustic energy. Thus, if the value of α increases, i.e., $\boldsymbol{z}_2$ is emphasized in the minimization process, total acoustic energy will be decreased. As such, the control performance will be tuned conveniently using only this scalar parameter.

Equations (13), (18), and (19) are combined and transformed into a state-space description for a generalized plant $\boldsymbol{G}(s)$ expressed as follows:

$$\left\{\begin{array}{l} \begin{Bmatrix} \dot{\boldsymbol{x}}_{\mathrm{a}} \\ \dot{\boldsymbol{x}}_{\mathrm{s}} \\ \dot{\boldsymbol{x}}_{\mathrm{p}} \end{Bmatrix} = \begin{bmatrix} \boldsymbol{A}_{\mathrm{a}} & \boldsymbol{0} & \boldsymbol{0} \\ \boldsymbol{0} & \boldsymbol{A}_{\mathrm{s}} & \boldsymbol{B}_{\mathrm{s}}\boldsymbol{C}_{\mathrm{e}} \\ \boldsymbol{0} & \boldsymbol{0} & \boldsymbol{A}_{\mathrm{p}} \end{bmatrix} \begin{Bmatrix} \boldsymbol{x}_{\mathrm{a}} \\ \boldsymbol{x}_{\mathrm{s}} \\ \boldsymbol{x}_{\mathrm{p}} \end{Bmatrix} + \begin{bmatrix} \boldsymbol{0} & \boldsymbol{0} \\ \boldsymbol{0} & \boldsymbol{0} \\ \boldsymbol{0} & \boldsymbol{B}_{\mathrm{w}} \end{bmatrix} \begin{Bmatrix} w_1 \\ \boldsymbol{w}_2 \end{Bmatrix} + \begin{Bmatrix} \boldsymbol{B}_{\mathrm{a}} \\ \boldsymbol{0} \\ \boldsymbol{B}_{\mathrm{p}} \end{Bmatrix} u \\ \begin{Bmatrix} z_1 \\ z_2 \end{Bmatrix} = \begin{bmatrix} \boldsymbol{C}_{\mathrm{a}} & \boldsymbol{0} & \boldsymbol{0} \\ \boldsymbol{0} & \alpha\boldsymbol{C}_{\mathrm{s}} & \boldsymbol{0} \end{bmatrix} \begin{Bmatrix} \boldsymbol{x}_{\mathrm{a}} \\ \boldsymbol{x}_{\mathrm{s}} \\ \boldsymbol{x}_{\mathrm{p}} \end{Bmatrix} + \begin{Bmatrix} D_{\mathrm{a}} \\ \boldsymbol{0} \end{Bmatrix} u \\ y = \{\boldsymbol{0}\ \boldsymbol{0}\ \boldsymbol{C}_{\mathrm{p}}\} \begin{Bmatrix} \boldsymbol{x}_{\mathrm{a}} \\ \boldsymbol{x}_{\mathrm{s}} \\ \boldsymbol{x}_{\mathrm{p}} \end{Bmatrix} + \{1\ 0\} \begin{Bmatrix} w_1 \\ \boldsymbol{w}_2 \end{Bmatrix} \end{array}\right. \tag{20}$$

Figure 7 shows a block diagram of the acoustic system including the above generalized plant and the feedback controller $K(s)$. The control system can be arranged as shown in Fig. 8. State-space description (20) allows us to obtain $K(s)$ for minimization of the total acoustic energy in a room through the state space approach explained in the previous section.

4. NUMERICAL STUDIES ON THE PROPOSED CONTROL METHOD

4.1. Conditions for Calculation

A computer simulation was performed to demonstrate the active minimization of the total acoustic energy in an enclosure. A lightly damped, two-dimensional model of a rectangular enclosure as illustrated in Fig. 9 was selected for the simulation. The primary and control sources were

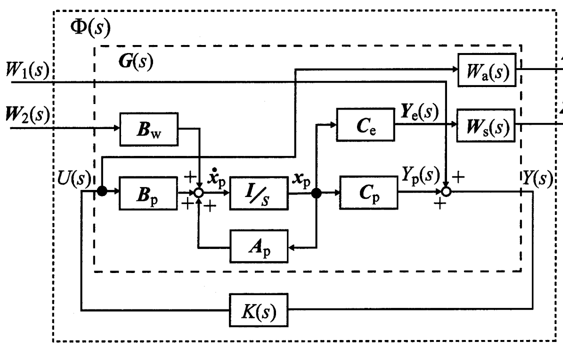

Fig. 7 Block diagram of acoustic system with feedback controller.

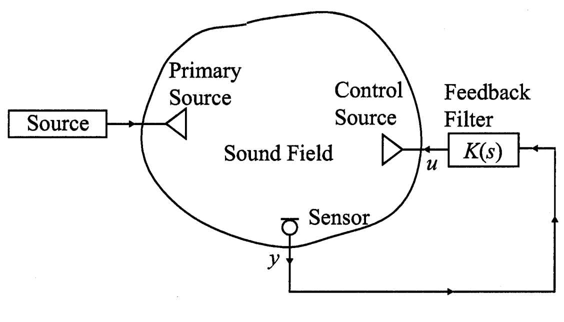

Fig. 8 Arrangement of sound field control system.

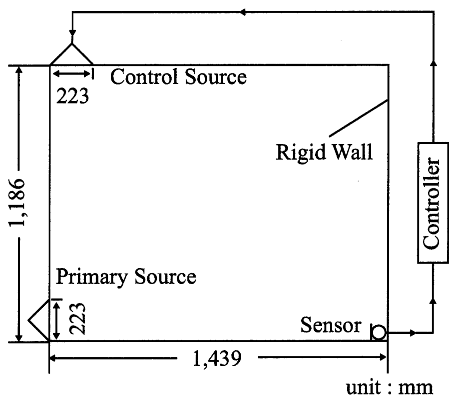

Fig. 9 Two-dimensional model of rectangular enclosure for computer simulations.

modeled as piston sources having uniform velocity distributions over their surfaces. The finite elements used to discretize the sound field were first-order, two-dimensional, isoparametric triangles. There were 960 such elements, assembled in 525 degrees of freedom. For calculating the damping matrix $\boldsymbol{D}$, it was assumed that the matrix could be transformed into a diagonal matrix using the undamped modal matrix, and damping ratios of 0.01 were assumed for all modes. The state equation for the sound field was then constructed by the method described in section 3.1. Since the high-order modes calculated by FEM are not accurate, the order of the state equation was reduced by modal reduction of the equation of motion of the multi-degree-of-freedom system expressed as Eq. (12). The initial coordinates of the 525 degrees were transformed into the modal coordinates of 7 degrees by

$$\boldsymbol{x}_{\mathrm{p}}{}' = \begin{Bmatrix} \boldsymbol{\xi} \\ \dot{\boldsymbol{\xi}} \end{Bmatrix} = \begin{bmatrix} \boldsymbol{\Psi}^{\mathrm{T}} & \boldsymbol{0} \\ \boldsymbol{0} & \boldsymbol{\Psi}^{\mathrm{T}} \end{bmatrix} \begin{Bmatrix} \boldsymbol{\phi} \\ \dot{\boldsymbol{\phi}} \end{Bmatrix} = \begin{bmatrix} \boldsymbol{\Psi}^{\mathrm{T}} & \boldsymbol{0} \\ \boldsymbol{0} & \boldsymbol{\Psi}^{\mathrm{T}} \end{bmatrix} \boldsymbol{x}_{\mathrm{p}}, \tag{21}$$

where $\boldsymbol{\Psi}$ is the undamped modal matrix containing only the 7 lowest eigenvectors without the rigid-body mode and $\boldsymbol{\xi}$ is a vector with components of the amplitude of each mode. The natural frequency of the 7th mode, which is the highest mode involved in the nominal model of the plant, is about 316 Hz. Thus, the weighting function $W_a(s)$ used for the design of the feedback controller was chosen as a 3rd-order Chebyshev high-pass filter with a cut-off frequency of 380 Hz and an allowable passband ripple of 0.5 dB. The other weighting function $\boldsymbol{W}_s(s)$ was chosen as a 2nd-order Butterworth low-pass filter with a cut-off frequency of 500 Hz.

In order to simulate the application of the present control method to a real sound field, a theoretical solution of the inhomogeneous wave equation (11) based on mode theory was adopted to express the dynamics of the real sound field. A state-space description of the sound field based on mode theory was constructed through the procedure given in the appendix. The highest mode involved in this state-space description is the 51st mode; the natural frequency of this mode is about 995 Hz. Coupling this state-space description simulating the real physical system with the state-space description of the designed feedback controller, the total acoustic energy in the sound field (also given in the appendix) was calculated. To assess the effectiveness of the proposed control method, feedback control by LQG was also performed on the theoretical basis presented in the previous paper [9].

4.2. Results and Discussion

Figure 10 shows the transient responses of the total acoustic energy in the sound field when the primary source is driven by the unit impulse function, for variations in the weighting factor α. It is demonstrated that, as α increases, the energy decays faster. The proposed active control of sound fields is classified into the control referred to as self-improvement via a minor loop, which has the functionality to change only the pole placement of the acoustic system. The real parts of the poles of the transfer function of the system dictate the rate at which the energy leaves the system. Thus, performing this control, formulated for the minimization of the total acoustic energy in an enclosure, the real parts of the poles of the transfer function are modified such that damping is increased. This indicates that the proposed control method can be used to actively tune the transient characteristics of a sound field, i.e., the reverberation time.

Figures 11–13 show the frequency spectrums of the total acoustic energy in the sound field for variations in the weighting factor α. Introducing the proposed control scheme, the energy is attenuated in the vicinity of the resonant frequencies below the natural frequency of the 7th mode. As α increases, the levels of attenuation are increased. The maximum reduction in the total acoustic energy is approximately 13 dB at the resonant frequency of the 1st mode. The most significant result is that in the frequency range above the natural frequency of the 8th mode, which is not involved in the nominal model of the plant, this control does not change the energy level. This result is difficult to obtain by ordinary control methods based on LQG, as shown in Fig. 14, where the energy of

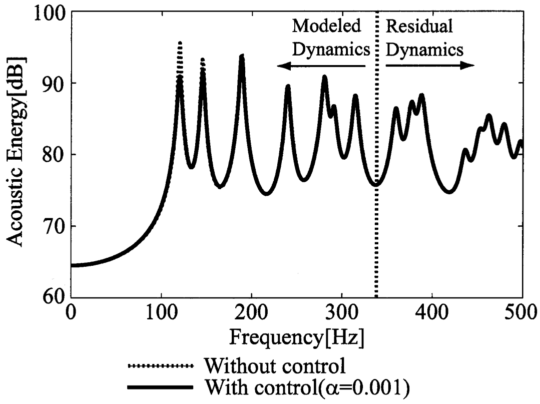

Fig. 11 Frequency spectrums of total acoustic energy in sound field with and without H_∞ control ($\alpha = 0.001$).

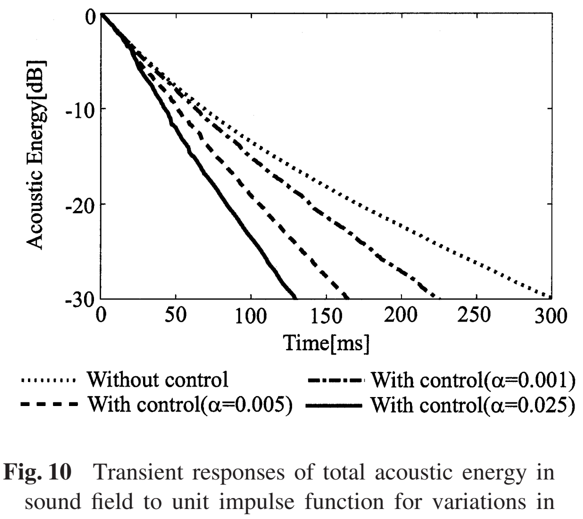

Fig. 10 Transient responses of total acoustic energy in sound field to unit impulse function for variations in weighting factor α of H_∞ control.

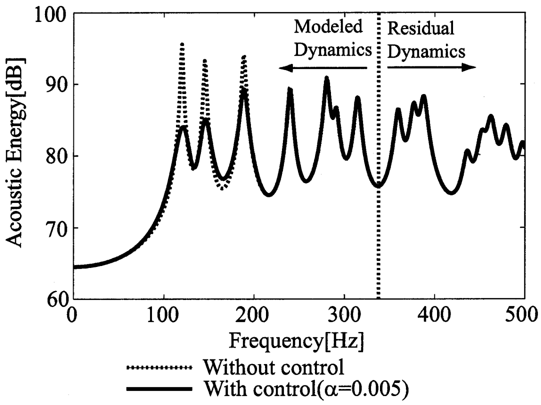

Fig. 12 Frequency spectrums of total acoustic energy in sound field with and without H_∞ control ($\alpha = 0.005$).

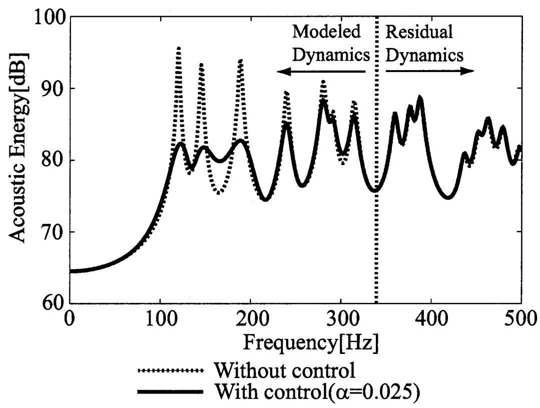

Fig. 13 Frequency spectrums of total acoustic energy in sound field with and without H_∞ control ($\alpha = 0.025$).

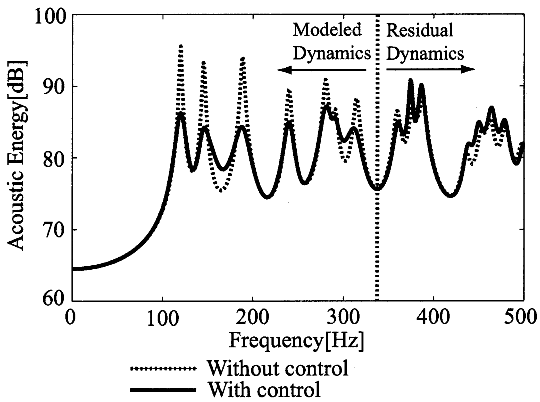

Fig. 14 Frequency spectrums of total acoustic energy in sound field with and without feedback control based on LQG.

the residual modes is amplified with the control. In addition, as mentioned previously, the proposed control method does not require a reference signal for the primary source to be supplied or the sound field to be harmonic. It only alters the dynamics of the sound field into which the control system introduced. Therefore, especially when a noise source is not periodic or its position varies with time, the present feedback control scheme based on H_∞ control theory is highly applicable to the minimization of the total acoustic energy in the sound field.

Although a small and regular shape enclosure was selected for the plant in this study, the proposed control method has ability to control three-dimensional domains with arbitrary sizes and shapes theoretically. However, if a sound field to be controlled is larger or has a more complicated geometry, more amounts of numerical calculations are required to obtain the feedback controller. The proposed control method uses FEM to identify a state equation for a sound field. When FEM is applied to model the dynamics of a sound field, the spatial scale of the sound field and the frequency range are restricted by computer performance such as memory capacity and processing speed. To represent the dynamics of a sound field accurately using FEM, the sound field under study must be discretized using small elements compared to the acoustic wavelength at the frequency of interest [19]. Thus, for a larger sound field or the higher-frequency range, the number of degrees of freedom of the sound field becomes larger. Recently, Otsuru *et al.* carried out an analysis of the sound field in an auditorium having the volume of about 12,000 m^3 in the frequency range lower than 500 Hz using FEM [20]. The resultant number of degrees of freedom was about 7,000,000. It is clear that a long processing time and large memory capacity are needed to construct the state equation of such a sound field.

The number of acoustic modes to be controlled is also restricted by computer performance. After modeling plant dynamics, the feedback controller is obtained using the solutions of two Riccati equations. When employing Potter's algorithm to solve the Riccati equations, the eignvalue problems of Hamiltonian matrices need to be solved [21]. The dimension of the Hamiltonian matrices is 2 times as large as the dimension of a state equation of a generalized plant. Thus, if a state equation involves more acoustic modes of a sound field, the order of computational complexity and the memory requirements become larger. In addition to this, since an eignvalue problem is generally sensitive to numerical errors, double precision arithmetic is required for the accuracy, causing that a computational load becomes high. Besides these computational aspects, the number of acoustic modes affects the practical implementation of the feedback controller. When the feedback controller is implemented on a DSP as an IIR filter, the dimension of the feedback controller is restricted by the processing speed of the DSP. The dimension of the controller is equal to the dimension of a state equation of a generalized plant. Thus, the performance of the DSP to be used determines the maximum number of acoustic modes that can be involved in a state equation.

According to these, the proposed control method requires that compromises are reached between keeping processing time to within acceptable limits, while including enough degrees of freedom to give an accurate modeling and including enough acoustic modes to give a broadband effect. At the present time, if a personal computer system is used to calculate the feedback controller, the proposed control method is suitable for control of relatively small sound fields such as automobile cabins and recording studios at low frequencies. It is not intended for control of large sound fields such as auditoriums and for control in the frequency range with high modal density in a practical application. An alternative method to model a sound field in a wide frequency range with the small number of degrees of freedom is expected to be developed in the field of sound field analysis to reduce the computational load.

5. CONCLUSIONS

In an effort to realize robust feedback control of a sound field of any shape, a method that links FEM with H_∞ control theory was proposed. The objective of control was minimization of the total acoustic energy in a sound field excited by unknown disturbances. The structure of the acoustic plant was formulated such that the H_∞ norm of the system transfer function expressed the total acoustic energy in the sound field.

Computer simulations demonstrated that the damping of the sound field can be increased without leading to instabilities of the closed loop system, and that the control performance can be tuned by changing the weighting factor. It was also demonstrated that the resonant peaks in the frequency spectrum of the total acoustic energy can be attenuated in the low-frequency range involved in the nominal model of the plant, while the residual plant dynamics in the high-frequency range are not unnecessarily excited.

This study discussed the plant uncertainty due to residual mode dynamics. Further investigation of plant uncertainties due to other factors such as boundary conditions may provide more attractive results in a practical control of a real sound field.

REFERENCES

[1] P. A. Nelson, A. R. D. Curtis, S. J. Elliott and A. J. Bullmore, "The active minimization of harmonic enclosed sound fields, part I: theory," *J. Sound Vib.*, **117**, 1–13 (1987).

[2] A. J. Bullmore, P. A. Nelson, A. R. D. Curtis and S. J. Elliott, "The active minimization of harmonic enclosed sound fields, part II: a computer simulation," *J. Sound Vib.*, **117**, 15–33 (1987).

[3] S. J. Elliott, A. R. D. Curtis, A. J. Bullmore and P. A. Nelson, "The active minimization of harmonic enclosed sound fields, part III: experimental verification," *J. Sound Vib.*, **117**, 35–58 (1987).

[4] S. Ise, S. Sakamoto and H. Tachibana, "Analysis of active mode control in a room by the boundary element method," *J. Acoust. Soc. Jpn. (J)*, **51**, 25–33 (1995).

[5] R. L. Clark and D. G. Cole, "Active damping of enclosed sound fields through direct rate feedback control," *J. Acoust. Soc. Am.*, **97**, 1710–1716 (1995).

[6] J. L. Dohner and R. Shoureshi, "Modal control of acoustic plants," *ASME J. Vib. Acoust. Stress, Reliab. Des.*, **111**, 326–330 (1989).

[7] M. R. Bai, C. Shieh and D. Lee, "Development of a modal LQG active noise canceler," *Proc. ACTIVE 95*, pp. 911–920 (1995).

[8] J. L. Dohner and R. Shoureshi, "A method for active noise control using a source-point model," *J. Acoust. Soc. Am.*, **86**, 1053–1059 (1989).

[9] T. Samejima and M. Yasuoka, "Active suppression of reverberation in a sound field through state feedback control," *J. Acoust. Soc. Jpn. (J)*, **55**, 12–22 (1999).

[10] M. J. Balas, "Feedback control of flexible systems," *IEEE Trans. Autom. Control*, **AC-23**, 673–679 (1978).

[11] B. A. Francis, *A Course in H_∞ Control Theory* (Springer-Verlag, Berlin, 1987).

[12] C. Foias, H. Özbay and A. Tannenbaum, *Robust Control of Infinite Dimensional Systems* (Springer-Verlag, Berlin, 1996).

[13] B. M. Chen, *H_∞ Control and Its Applications* (Springer-Verlag, Berlin, 1998).

[14] M. Sampei and T. Mita, "A state space approach to H^∞ control problems," *J. Soc. Instrum. Control Eng.*, **29**, 129–135 (1990).

[15] Y. Kagawa, T. Yamabuchi and A. Mori, "Finite element simulation of an axisymmetric acoustic transmission system with a sound absorbing wall," *J. Sound Vib.*, **53**, 357–374 (1977).

[16] A. Craggs, "The application of acoustic and absorption finite elements to sound fields in small enclosures," in *Finite Element Applications in Acoustics*, M. M. Kamal and J. A. Wolf, Jr., Eds. (ASME, New York, 1981), pp. 1–19.

[17] T. Samejima, "System modeling of a sound field including mechanism of a loudspeaker and state feedback control of it," *Proc. Spring Meet. Acoust. Soc. Jpn.*, pp. 519–520 (1999).

[18] The Architectural Institute of Japan, *Prediction of Sound Field in Rooms: Theory, Application and Recent Development* (The Architectural Institute of Japan, Tokyo, 2001), pp. 86–88.

[19] T. Samejima, K. Hirate and M. Yasuoka, "State-space expression of a sound field by theoretical or experimental identification of it," *J. Archit. Plann. Environ. Eng.*, **515**, 9–16 (1999).

[20] T. Otsuru and R. Tomiku, "Finite element sound field analysis of rooms with large scale—Basic investigation on multi-frequency analysis—," *Proc. Autumn Meet. Acoust. Soc. Jpn.*, pp. 955–956 (2001).

[21] J. E. Potter, "Matrix quadratic solutions," *J. SIAM Appl. Math.*, **14**, 496–501 (1966).

APPENDIX: STATE-SPACE DESCRIPTION OF A SOUND FIELD BASED ON MODE THEORY

The proposed procedure for constructing a state equation for a sound field based on the theoretical analysis of the inhomogeneous wave equation (11) using mode theory is as follows.

According to mode theory, the velocity potential ϕ in an enclosure can be expressed in modal coordinates such that

$$\phi = \sum_{n=1}^{\infty} \eta_n(t)\psi_n(x, y, z), \tag{A·1}$$

where $\psi_n(x, y, z)$ and $\eta_n(t)$ are a characteristic function and modal response of the n-th mode, respectively. For a rectangular enclosure, the characteristic functions are given by

$$\psi_n = \varepsilon_n \cos\left(\frac{n_x \pi x}{L_x}\right) \cos\left(\frac{n_y \pi y}{L_y}\right) \cos\left(\frac{n_z \pi z}{L_z}\right), \tag{A·2}$$

where n_x, n_y, and n_z are integers, L_x, L_y, and L_z are the dimensions of the enclosure. With the normalization factors ε_n, the characteristic functions are normalized such that

$$\iiint_{\Omega} \psi_n \psi_m dV = L_x L_y L_z \delta_{nm} = V\delta_{nm}, \tag{A·3}$$

where V is the volume of the enclosure. Substituting Eq. (A·1) into Eq. (11) and using the orthogonality of Eq. (A·3), one can obtain

$$\frac{\partial^2 \eta_n}{\partial t^2} + {\omega_n}^2 \eta_n = \frac{c^2}{V} \iiint_{\Omega} q\psi_n dV, \tag{A·4}$$

with

$${\omega_n}^2 = c^2 \left\{ \left(\frac{n_x \pi}{L_x}\right)^2 + \left(\frac{n_y \pi}{L_y}\right)^2 + \left(\frac{n_z \pi}{L_z}\right)^2 \right\}, \tag{A·5}$$

where ω_n is the natural angular frequency of the n-th mode. Assuming that the enclosure is lightly damped and introducing a modal damping ratio ζ_n,

$$\frac{\partial^2 \eta_n}{\partial t^2} + 2\zeta_n \omega_n \frac{\partial \eta_n}{\partial t} + {\omega_n}^2 \eta_n = \frac{c^2}{V} \iiint_{\Omega} q\psi_n dV. \tag{A·6}$$

Equation (A·6) can be transformed into a state-space description as follows:

$$\begin{cases} \dot{\boldsymbol{x}}_{\mathrm{r}} = \boldsymbol{A}_{\mathrm{r}} \boldsymbol{x}_{\mathrm{r}} + \boldsymbol{B}_{\mathrm{rp}} u_{\mathrm{p}} + \boldsymbol{B}_{\mathrm{rs}} u_{\mathrm{s}} \\ y_{\mathrm{r}} = \boldsymbol{c}_{\mathrm{r}} \boldsymbol{x}_{\mathrm{r}} \end{cases}, \tag{A·7}$$

with

$$\begin{aligned}
\boldsymbol{A}_{\mathrm{r}} &= \begin{bmatrix} \boldsymbol{0} & \boldsymbol{I} \\ -\operatorname{diag}[{\omega_n}^2] & -\operatorname{diag}[2\zeta_n \omega_n] \end{bmatrix}, \boldsymbol{x}_{\mathrm{r}} = \begin{Bmatrix} \boldsymbol{\eta} \\ \dot{\boldsymbol{\eta}} \end{Bmatrix}, \\
\boldsymbol{B}_{\mathrm{rp}} &= \begin{Bmatrix} \boldsymbol{0} \\ \boldsymbol{q}_{\mathrm{p}} \end{Bmatrix}, \boldsymbol{q}_{\mathrm{p}} = \frac{c^2}{V} \left\{ \iiint_{\Omega_{\mathrm{p}}} \psi_1 dV \iiint_{\Omega_{\mathrm{p}}} \psi_2 dV \cdots \iiint_{\Omega_{\mathrm{p}}} \psi_N dV \right\}^{\mathrm{T}}, \\
\boldsymbol{B}_{\mathrm{rs}} &= \begin{Bmatrix} \boldsymbol{0} \\ \boldsymbol{q}_{\mathrm{s}} \end{Bmatrix}, \boldsymbol{q}_{\mathrm{s}} = \frac{c^2}{V} \left\{ \iiint_{\Omega_{\mathrm{s}}} \psi_1 dV \iiint_{\Omega_{\mathrm{s}}} \psi_2 dV \cdots \iiint_{\Omega_{\mathrm{s}}} \psi_N dV \right\}^{\mathrm{T}}, \\
\boldsymbol{c}_{\mathrm{r}} &= \rho \{ \boldsymbol{0} \quad \psi_1(\boldsymbol{r}) \psi_2(\boldsymbol{r}) \cdots \psi_N(\boldsymbol{r}) \},
\end{aligned}$$

where u_{p} and u_{s} are the strength of the primary source and control source, $\boldsymbol{\eta}$ is a vector with components of η_n, and Ω_{p} and Ω_{s} denote the area of the primary source and control source. It is assumed that one can achieve a reasonably accurate representation of the sound field with a finite value of N though $N = \infty$ in theory. The output equation is formulated such that the output y_{r} of the system becomes the sound pressure at a point $\boldsymbol{r}$ in the sound field.

Using the above state space variables $\boldsymbol{x}_{\mathrm{r}}$, the instantaneous total acoustic energy in the sound field is expressed as

$$\begin{aligned}
E &= \frac{\rho V}{2c^2} \sum_{n=1}^{N} {\omega_n}^2 {\eta_n}^2 + \frac{\rho V}{2c^2} \sum_{n=1}^{N} {\dot{\eta}_n}^2 \\
&= \boldsymbol{\eta}^{\mathrm{T}} \frac{\rho V}{2c^2} \operatorname{diag}[{\omega_n}^2] \boldsymbol{\eta} + \dot{\boldsymbol{\eta}}^{\mathrm{T}} \frac{\rho V}{2c^2} \boldsymbol{I} \dot{\boldsymbol{\eta}} \\
&= {\boldsymbol{x}_{\mathrm{r}}}^{\mathrm{T}} \begin{bmatrix} \frac{\rho V}{2c^2} \operatorname{diag}[{\omega_n}^2] & \boldsymbol{0} \\ \boldsymbol{0} & \frac{\rho V}{2c^2} \boldsymbol{I} \end{bmatrix} \boldsymbol{x}_{\mathrm{r}}.
\end{aligned} \tag{A·8}$$